Pushing the limits of beam-steering lens arrays

Håkon J. D. Johnsen, Astrid Aksnes, Jan Torgersen

Håkon J. D. Johnsen, Astrid Aksnes, Jan Torgersen, "Pushing the limits of beam-steering lens arrays," Proc. SPIE 11120, Nonimaging Optics: Efficient Design for Illumination and Solar Concentration XVI, 111200B (9 September 2019); doi: 10.1117/12.2528751

SPIE.

Event: SPIE Optical Engineering + Applications, 2019, San Diego, California, United States

Pushing the limits of beam-steering lens arrays

Håkon J. D. Johnsen*[a], Astrid Aksnes[b], and Jan Torgersen[a]

[a]Department of Mechanical and Industrial Engineering, Norwegian University of Science and Technology, Trondheim, Norway
[b]Department of Electronic Systems, Norwegian University of Science and Technology, Trondheim, Norway

ABSTRACT

An essential part of a concentrated solar power system is the solar tracker. Tracking is usually implemented by rotating the entire optical system to follow the sun, adding to the bulk and complexity of the system. Beam-steering lens arrays, on the other hand, enable solar tracking using millimeter-scale relative translation between a set of lens arrays stacked in an afocal configuration. We present an approach for designing and comparing beam-steering lens arrays based on multi-objective optimization, where the objective is to maximize efficiency, minimize divergence, and minimize cost/complexity. We then use this approach to develop new configurations with improved performance compared to previously reported results. As an example of a design suitable for high-concentration applications, we present a system consisting of four single-sided lens arrays that can track the sun with a yearly average efficiency of 74.4% into an exit-cone with divergence half-angle less than $\pm 1^\circ$. We also present a simplified system consisting of three single-sided lens arrays, which can be implemented with less mechanical complexity and potentially lower cost. This simplified system achieves 74.6% efficiency and a divergence half-angle of less than $\pm 2.2^\circ$, and might be relevant for low or medium concentration applications. We believe that these results demonstrate the previously untapped potential of beam-steering lens arrays. If such designs are successfully manufactured, they may become an attractive alternative to conventional external solar trackers for a range of solar energy applications.

Keywords: beam-steering, lens arrays, solar tracking, micro-tracking

1 INTRODUCTION

Solar concentrators can provide highly concentrated solar power for applications such as concentrator photovoltaics, solar thermal energy, or solar lighting.[1] The concentrators require accurate solar tracking in order to achieve high concentration,[2] which is usually performed by rotating the concentrator to face the sun. Recent work, however, has considered the use of tracking-integrated systems, which can track the sun without being rotated by an external solar tracker.[3]

One approach to tracking-integration is the concept of beam-steering, where a tracking-integrated system emits collimated light, which can then be concentrated in a separate concentrator, as conceptually illustrated in Figure 1a. This approach enables the same beam-steering system to be used for several different applications and allows the design of the concentrator optics to be independent of the design of the tracking optics. Several beam-steering concepts have been proposed for solar tracking, including electrowetting to change the angle of the interface between two liquids with different refractive indices,[4] microfluidic beam-steering arrays,[5] rotating prism arrays,[6] liquid crystals controlled by electric fields,[7] rotating off-axis Fresnel lenses,[8] and beam-steering lens arrays.[9,10]

A beam-steering lens array consists of a set of lens arrays stacked in an afocal configuration that can redirect sunlight by relative movement between these lens arrays, as first proposed for solar tracking by Lin et al.[9] The core principle is illustrated in Figure 1b.

In this work, we investigate the achievable performance of beam-steering lens arrays. We develop a new approach for comparing different beam-steering lens array configurations and use it to optimize new configurations with improved performance compared to previously reported results.

* E-mail: hakon.j.d.johnsen@ntnu.no

Nonimaging Optics: Efficient Design for Illumination and Solar Concentration XVI, edited by Roland Winston, Eli Yablonovitch, Proc. of SPIE Vol. 11120, 111200B · © 2019 SPIE
CCC code: 0277-786X/19/$21 · doi: 10.1117/12.2528751

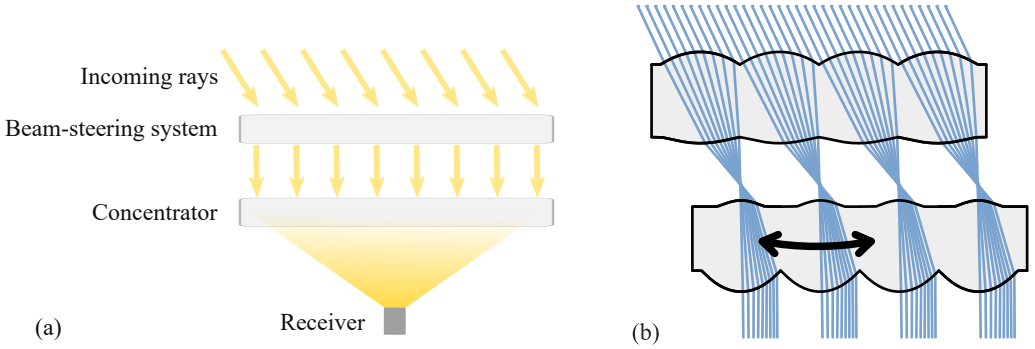

Figure 1: (a) Conceptual illustration of how a beam-steering system can be combined with conventional concentrator optics. (b) Example of a beam-steering lens array: An afocal stack of lens arrays, which redirects sunlight utilizing relative movement between these lens arrays.

2 CLASSIFYING DIFFERENT CONFIGURATIONS

With the development of new types of beam-steering lens arrays, we believe that it will be useful to have a way of classifying different designs. Previous beam-steering lens array designs have utilized both single-sided[9] and double-sided[10] lens arrays, with relative lateral[11] or curved[9] tracking motion, and with both two,[9] and three[12] lens arrays stacked together. In order to readily specify, compare, and evaluate different classes of designs, it can be useful to designate specific symbols for each of the components in a beam-steering lens array. Specific configurations of beam-steering lens arrays can then be described using a sequence of these symbols.

In this work, we use the set of symbols shown in Table 1.

Table 1: Proposed symbols for classifying different beam-steering lens array configurations. Symbols are represented in Unicode and can be copied and pasted as text into any software that supports Unicode.

Symbol*	Meaning
◀	Single-sided lens array with the flat side on the right.
▶	Single-sided lens array with the flat side on the left.
◆	Double-sided lens array
↓	Air-gap between lens arrays supporting a flat, lateral tracking trajectory.
⤸	Air-gap between lens arrays supporting a curved tracking trajectory.
◀▶	A pair of single-sided lens arrays placed back-to-back, with index-matched lubricating oil between them supporting relative lateral translation between the lens arrays.

The symbols from Table 1 can be used to classify both existing and new beam-steering lens array configurations. For instance:

- Lin et al., 2012:[9] ◀⤸▶
- Watson, 1993[14] (for steering of laser beams): ◆↓◆and ◆↓◆ ◆
- Johnsen et al., 2018:[10] ◆⤸◆and ◀⤸◆⤸◆

*The symbols are represented by the following Unicode[13] code-points: ◀=U+25C0, ▶=U+25B6, ◆=U+25C6, ↓=U+2193, ⤸=U+2938, ◀▶=U+25C0 U+200A U+25B6

3 DESIGN METHOD

We have utilized a design method based on ray-tracing and numerical optimization for designing and comparing different beam-steering lens array configurations. In this section, we describe this design method and specify the conditions for the optimization results reported in this paper.

3.1 Formulation of the optimization problem

We consider three main performance objectives for evaluating the performance of a complete beam-steering lens array:

- Maximizing the efficiency in redirecting sunlight.
- Minimizing the divergence of outgoing sunlight
- Minimizing the cost/complexity

The design of a beam-steering lens array can, therefore, be considered a multi-objective optimization problem. An optimal solution must provide a reasonable trade-off between these objectives. Multi-objective optimization problems can be solved by finding a set of Pareto optimal solutions: solutions where one objective cannot be improved without degrading another objective. In this way, the trade-off between objectives is quantified, allowing a designer to make an informed choice among the set of solutions.[15]

Efficiency and divergence can be quantified as continuous objective values, allowing a multi-objective optimization algorithm to map out the Pareto front between these objectives. Cost/complexity, on the other hand, is difficult to quantify and depends on several different factors. We have, therefore, not tried to quantify complexity directly. Instead, we optimized several different configurations with different levels of complexity.

We formulated the following optimization problem:

$$\min \mathbf{f}(\mathbf{x}, \theta_{max}) = \left(1 - \overline{\eta}\left(\mathbf{x}, \theta_{max}\right), \theta_{max}\right)^T \tag{1}$$

$$\text{such that } g_j(\mathbf{x}) \leq 0, \tag{2}$$

where θ_{max} is the allowed divergence of outgoing sunlight, and $\overline{\eta}(\mathbf{x}, \theta_{max})$ is the average yearly optical efficiency of the optical system $\mathbf{x}$. $g_j(\mathbf{x})$ is a set of inequality constraints, ensuring manufacturability.

3.2 Estimating average optical efficiency

Average optical efficiency can be defined as the fraction of yearly direct irradiation successfully redirected in the desired direction:

$$\overline{\eta}\left(\mathbf{x}, \theta_{max}\right) = \frac{E_{out}\left(\mathbf{x}, \theta_{max}\right)}{E_{in}}, \tag{3}$$

where E_{in} is the yearly direct irradiation received by the beam-steering lens array surface, and $E_{out}(\mathbf{x}, \theta_{max})$ is the yearly irradiation successfully redirected within the permitted exit cone.

This average efficiency can be estimated by integrating across all angles of incidence:

$$\bar{\eta}\left(\mathbf{x}, \theta_{max}\right) = \int_0^{\pi} e(\phi) \cdot \eta\left(\mathbf{x}, \theta_{max}, \phi\right) d\phi, \tag{4}$$

where $e(\phi) = \frac{E_{in,\phi}(\phi)}{E_{in}}$ is the normalized angular distribution of irradiation received by the beam-steering lens array in its installation location. $\eta(\mathbf{x}, \theta_{max}, \phi)$ is the optical efficiency of the beam-steering lens for an optical system $\mathbf{x}$, a maximum divergence of outgoing sunlight θ_{max} and an angle of incidence ϕ.

In this work, we consider the beam-steering lens arrays to have a fixed orientation, tilted towards the equator with an angle equal to the latitude of the installation location as illustrated in Figure 2a. As noted by Ito et al., this orientation gives a peak in irradiation distribution at $22° - 25°$ angle of incidence, irrespective of installation location.[16] We consider the beam-steering lens arrays optimized in this paper to be installed at a latitude of 40°. We simulate the angular distribution of solar irradiation using Meinel and Meinel's air mass attenuation model[17] and assuming that cloud cover is not correlated to time of day or time of year. The resulting normalized irradiation distribution is shown in Figure 2b. When planning a physical realization of such a system, the real meteorological conditions of the desired installation location should be used.

It is worth noting that $\bar{\eta}$ in Equation 3 is defined relative to the irradiation reaching the front surface of the beam-steering lens array as it is mounted in its assumed orientation. Cosine projection loss is therefore not included in this average efficiency, and will give an additional reduction in power compared to a system pointed directly towards the sun. On the other hand, fixed-orientation systems can increase power conversion per land area due to reduced shading between modules, as discussed by Price et al.[18] These effects must be taken into account when comparing tracking-integrated systems to externally tracked systems, but have been considered to be beyond the scope of this work.

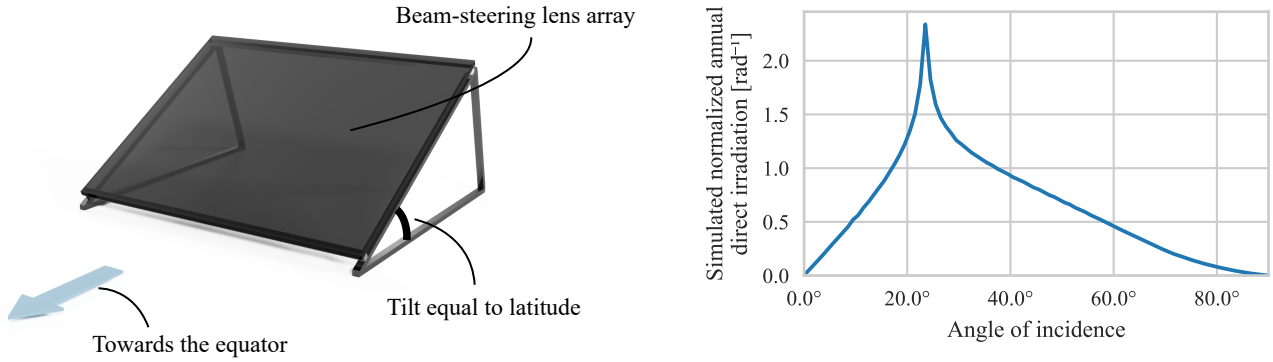

(a) (b)

Figure 2: (a) Assumed orientation of beam-steering lens array during optimization. (b) Simulated angular distribution of normalized yearly direct irradiation on a lens array with the fixed orientation from a, installed at a latitude of 40°

3.3 Numerical optimization

The multi-objective optimization problem in Equation 1 is trivially scalarized by setting a fixed θ_{max}. The Pareto front can then be mapped by repeated optimization of the resulting single-objective optimization problem for different values of θ_{max}.

The scalarized optimization problem was solved using a custom memetic optimization algorithm inspired by Qin et al.'s local search chains.[19] The differential evolution solver from SciPy[20] was extended to optimize the population using local search chains based on SciPy's SLSQP optimization algorithm in addition to the global differential evolution algorithm. The memetic optimization algorithm was run for 1500 iterations for each combination of beam-steering lens array configuration and permitted divergence half-angle, which seemed to give a reasonable trade-off between convergence and computational resources.

The optimization routine was implemented in a Jupyter Notebook[21] and parameterized using Papermill.[22] The optimization workflow was managed using Snakemake,[23] and solved using computational resources from Google Compute Engine. Ray-tracing was performed using a custom sequential three-dimensional ray-tracer, as reported in previous work.[10] Hexagonal lens apertures were used for all simulations to simulate close packing in a lens array. Optimizations were performed across the AM1.5D solar spectrum,[24] and all lenses were assumed to be made from Poly(methyl methacrylate) (PMMA). Reflection losses and chromatic aberration were taken

into account, while absorption losses were not considered.[†] Sunlight was assumed to originate from a uniform solar disc with a 0.27° angular radius. Average efficiency according to Equation 4 was estimated using multi-dimensional numerical integration with a quasi-Monte Carlo method and a low-discrepancy Sobol sequence. Lens surfaces were represented as Forbes' Q^{con} surfaces,[25] with a curvature, a conic constant, and 3 Q^{con} polynomial terms.

Four different configurations were optimized across a range of permitted divergence half-angles from ±0.3° to ±4°: ◀▶⤸◀▶ was optimized to evaluate achievable performance with the most complex configuration with up to 4 air-interfaces. ◀▶↓▶ was optimized to evaluate achievable performance with a simplified and potentially lower-cost system. ◀⤸◆⤸◆ and ◆⤸◆ were optimized for comparison, because they have previously been shown to have good performance for solar tracking.[10]

In each design, the lateral movements of the different lens arrays were constrained to be proportional to each other, allowing linked control, sharing the same mechanical actuator. The aspect ratio of each lens surface was constrained to be 0.7 or less, to prevent excessively curved lenses. Each lens array was constrained not to be thinner than half the lenslet diameter, to prevent too thin lens arrays.

4 RESULTS AND DISCUSSION

Equation 1 was solved using numerical optimization, as described in Section 3.3. The result is shown in Figure 3. Each line represents a specific beam-steering lens array configuration and shows the optimized yearly average efficiency for this configuration as a function of permitted divergence half-angle. Given the non-convex nature of the optimization problem, the optimization algorithm is not guaranteed to find the global optimum. The resulting Pareto front therefore only gives a lower bound on achievable efficiency for a specific configuration and divergence half-angle.

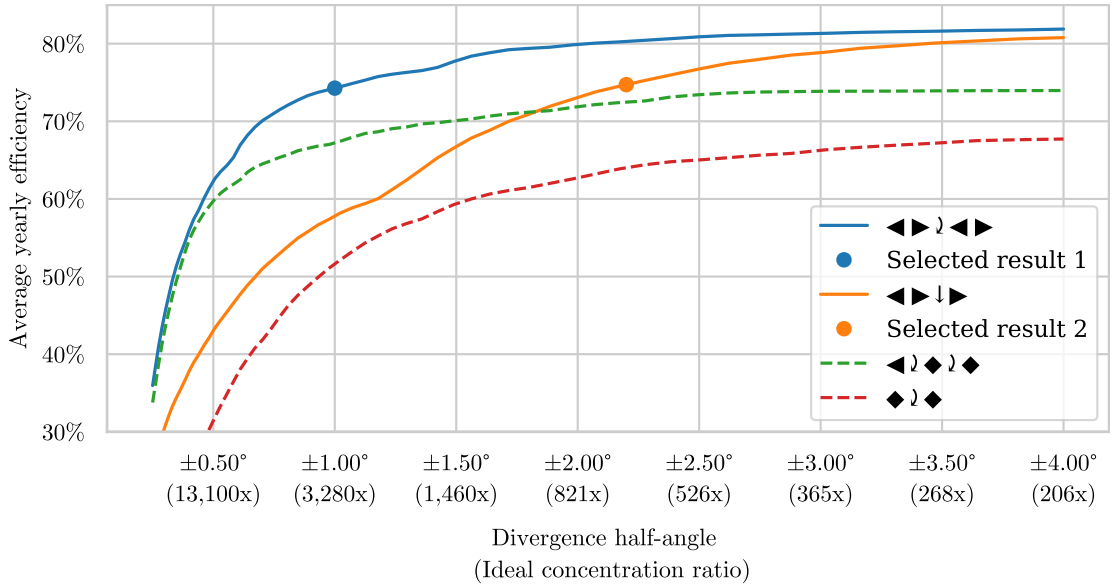

Figure 3: Optimized yearly efficiency as a function of permitted divergence half-angle for different configurations. For reference, the x-axis also shows the corresponding concentration ratio for an ideal concentrator at the given divergence half-angle.

4.1 Selected results

We choose to highlight two results that we believe to be of interest for solar energy applications. The first result is a ◀▶⤸◀▶ configuration optimized for a divergence half-angle of ±1°, which achieves 74.4% average yearly

[†]The beam-steering lens array is a scale-invariant afocal system (as long as it is operated far away from the diffraction limit). Absorption losses depend on the dimensions of the system, which were not specified in these simulations.

efficiency. This configuration, which may be relevant for high concentration applications, such as concentrator photovoltaics (CPV) or solar thermophotovoltaics, is highlighted with a blue circle in the Pareto front in Figure 3. A ray-traced drawing of the system can be seen in Figure 4. Simulated efficiency across the tracking range is shown in Figure 6a and is overlaid with a yearly irradiation distribution in Figure 6b.

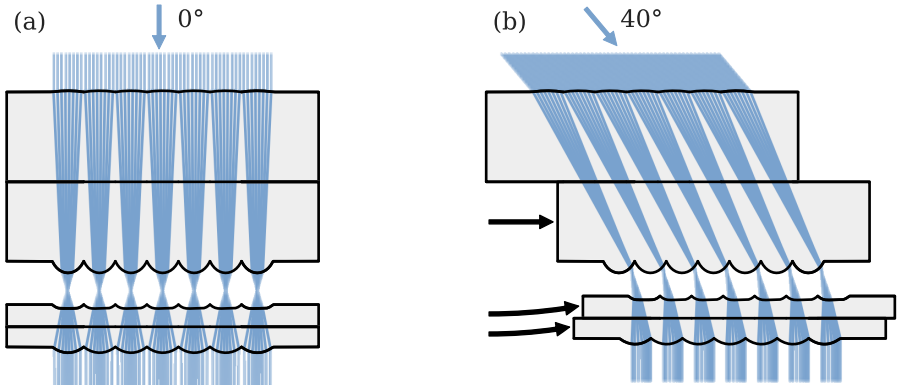

Figure 4: Beam-steering lens array with ◀▶⤸◀▶ configuration optimized for 1° divergence half-angle at (a) 0° angle of incidence and (b) 40° angle of incidence. Tracking motion is indicated by black arrows.

The second highlighted result is a ◀▶↓▶ configuration optimized for ±2.2° divergence half-angle. This configuration offers simpler mechanical implementation at the cost of lower optical performance. Compared to the previous result, the number of single-sided lens arrays is reduced from 4 to 3, and all relative motion is strictly lateral. This result is highlighted with an orange circle in the Pareto front in Figure 3, and a ray-traced drawing of the system can be seen in Figure 5. Simulated efficiency across the tracking range is shown in Figure 6a, and is overlaid with a yearly irradiation distribution in Figure 6b. This configuration may be relevant for medium concentration applications, such as concentrated solar power (CSP), or for solar lighting applications. The sine limit of concentration[26] for an ideal concentrator placed behind this beam-steering lens array is $678x$, which is more than three times the $212x$ ideal concentration ratio for a trough concentrator with single-axis tracking. This indicates that such a simplified beam-steering lens array can be useful for CSP applications despite the relaxed divergence requirements.

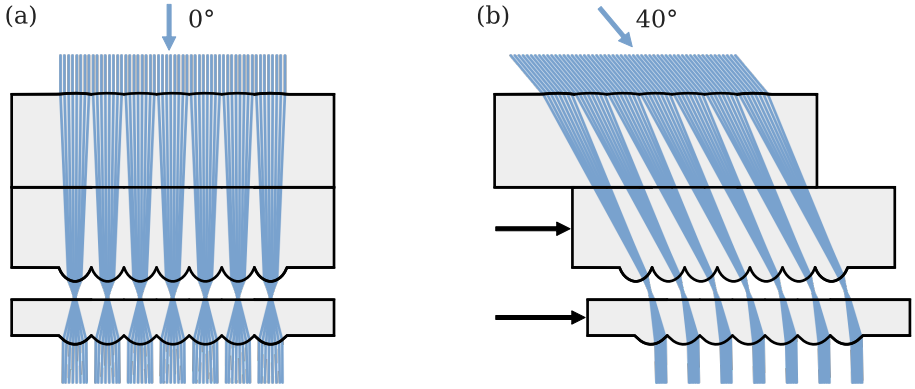

Figure 5: Simplified beam-steering lens array with ◀▶↓▶ configuration optimized for 2.2° divergence half-angle at (a) 0° angle of incidence and (b) 40° angle of incidence. Tracking motion is indicated by black arrows.

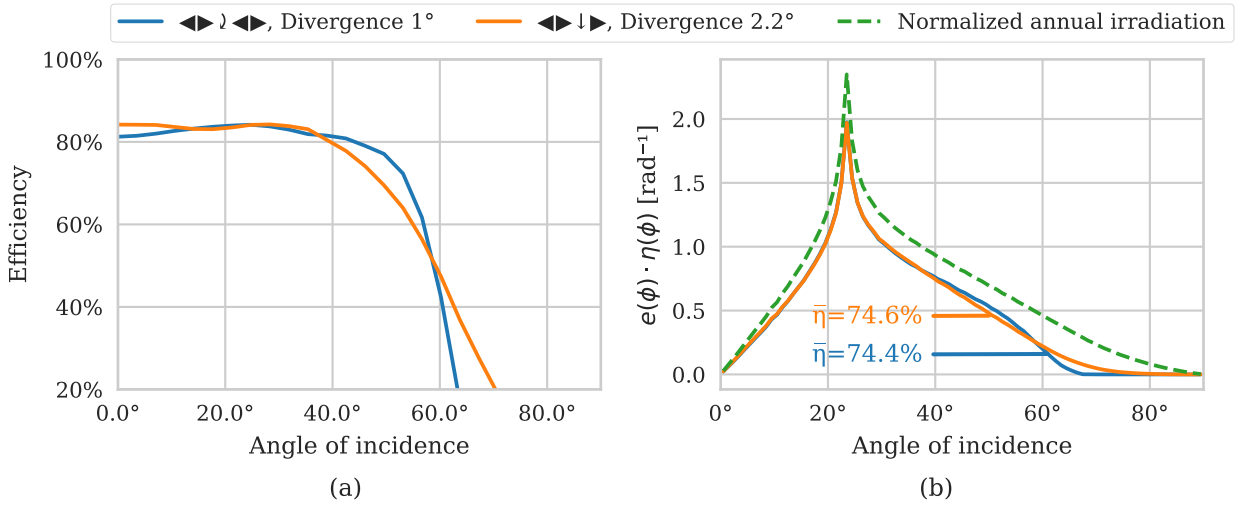

Figure 6: (a) The two selected beam-steering lens arrays have >80% efficiency for ±40°angle of incidence, and a gradual drop-off in efficiency at larger angles of incidence. (b) When the systems are placed in a fixed orientation as described in Section 3.2, this efficiency distribution corresponds to average yearly efficiency of 74.4% for the high concentration design and 74.6% for the simplified design, respectively.

5 CONCLUSIONS

We have introduced a set of symbols for categorizing different beam-steering lens array configurations and developed a numerical approach based on multi-objective optimization for comparing the performance of different configurations depending on application requirements. Using this approach, we have identified new configurations of beam-steering lens arrays that, to the best of our knowledge, outperform previous beam-steering lens arrays reported in the literature. Further work will involve a more extensive search through possible beam-steering lens array configurations, and exploration of the consequences for other installation orientation and locations as well as real-world manufacturing tolerances. The beam-steering lens array configurations reported in this paper may contribute to low-cost tracking-integrated solar energy, and the multi-objective optimization approach may enable further developments in this field. The presented designs are compatible with high-volume manufacturing methods such as injection molding, and future work may also involve extending the concept to Fresnel lenses compatible with roll-to-roll manufacturing processes such as extrusion coating.[27]

REFERENCES

[1] Xie, W. T., Dai, Y. J., Wang, R. Z., and Sumathy, K., "Concentrated solar energy applications using Fresnel lenses: A review," *Renewable and Sustainable Energy Reviews* **15**(6), 2588–2606 (2011).

[2] Winston, R., Minano, J. C., Benitez, P. G., contributions by Narkis Shatz and John C. Bortz, W., and Bortz, J. C., [*Nonimaging Optics*], Elsevier Science (2005).

[3] Apostoleris, H., Stefancich, M., and Chiesa, M., "Tracking-integrated systems for concentrating photovoltaics," *Nature Energy* **1**, 16018 (2016).

[4] Narasimhan, V., Jiang, D., and Park, S.-Y., "Design and optical analyses of an arrayed microfluidic tunable prism panel for enhancing solar energy collection," *Applied Energy* **162**, 450–459 (2016).

[5] DiDomenico, L. D., "Towards doubling solar harvests using wide-angle, broad-band microfluidic beam steering arrays," *Optics Express* **23**(24), A1398–A1417 (2015).

[6] León, N., Ramírez, C., and García, H., "Rotating Prism Array for Solar Tracking," *Energy Procedia* **57**, 265–274 (2014).

[7] Valyukh, S., Valyukh, I., and Chigrinov, V., "Liquid-Crystal Based Light Steering Optical Elements," *Photonics Letters of Poland* **3**(2), 88–90 (2011).

[8] Campbell, R. and Machado, M., "LOW cost CPV = Embedded CPV with internal tracker," in [*2010 35th IEEE Photovoltaic Specialists Conference (PVSC)*], 003003–003007 (2010).

[9] Lin, W., Benitez, P., and Miñano, J. C., "Beam-steering array optics designs with the SMS method," *Proc. SPIE* **8485**, 848505–848505–7 (2012).

[10] Johnsen, H. J. D., Torgersen, J., and Aksnes, A., "Solar tracking using beam-steering lens arrays," *Proc. SPIE* **10758**, 1075805, International Society for Optics and Photonics (2018).

[11] Watson, E., Miller, D., and Barnard, K., "Analysis of fill factor improvement using microlens arrays," *Proc. SPIE* **3276**, 123–134 (1998).

[12] Duparré, J., Radtke, D., and Dannberg, P., "Implementation of field lens arrays in beam-deflecting microlens array telescopes," *Applied Optics* **43**(25), 4854–4861 (2004).

[13] Unicode Consortium, [*The Unicode Standard, Version 12.0*] (2019).

[14] Watson, E. A., "Analysis of beam steering with decentered microlens arrays," *Optical Engineering* **32**(11), 2665–2670 (1993).

[15] Pardalos, P. M., Žilinskas, A., and Žilinskas, J., [*Non-Convex Multi-Objective Optimization*], Springer Optimization and Its Applications, Springer International Publishing (2017).

[16] Ito, A., Sato, D., and Yamada, N., "Optical design and demonstration of microtracking CPV module with bi-convex aspheric lens array," *Optics Express* **26**(18), A879–A891 (2018).

[17] Meinel, A. B. and Meinel, M. P., [*Applied Solar Energy: An Introduction*], Addison-Wesley (1976).

[18] Price, J. S., Sheng, X., Meulblok, B. M., Rogers, J. A., and Giebink, N. C., "Wide-angle planar microtracking for quasi-static microcell concentrating photovoltaics," *Nature Communications* **6**, 6223 (2015).

[19] Qin, A. K., Tang, K., Pan, H., and Xia, S., "Self-adaptive differential evolution with local search chains for real-parameter single-objective optimization," in [*2014 IEEE Congress on Evolutionary Computation (CEC)*], 467–474, IEEE, Beijing, China (2014).

[20] Jones, E., Oliphant, T., Peterson, P., et al., "SciPy: Open source scientific tools for Python," (2001).

[21] Thomas, K., Benjamin, R.-K., Fernando, P., Brian, G., Matthias, B., Jonathan, F., Kyle, K., Jessica, H., Jason, G., Sylvain, C., Paul, I., Damián, A., Safia, A., Carol, W., and Team, J. D., "Jupyter Notebooks – a publishing format for reproducible computational workflows," in [*ELPUB*], 87–90 (2016).

[22] nteract team, "Welcome to papermill — papermill 1.0.1 documentation." https://papermill.readthedocs.io/en/latest/ (2019).

[23] Köster, J. and Rahmann, S., "Snakemake—a scalable bioinformatics workflow engine," *Bioinformatics* **28**(19), 2520–2522 (2012).

[24] Renewable Resource Data Center, "Solar Spectral Irradiance: Air Mass 1.5." https://rredc.nrel.gov/solar/spectra/am1.5/.

[25] Forbes, G. W., "Shape specification for axially symmetric optical surfaces," *Optics express* **15**(8), 5218–5226 (2007).

[26] Winston, R., Jiang, L., and Ricketts, M., "Nonimaging optics: A tutorial," *Advances in Optics and Photonics* **10**(2), 484–511 (2018).

[27] Steinberg, C., Al-Hussainawi, N., Papenheim, M., Mayer, A., Scheer, H.-C., Matschuk, M., and Pranov, H., "Low reflection Fresnel lenses via double imprint combined with vacuum-UV surface hardening," *Journal of Vacuum Science & Technology B* **35**(6), 06G306 (2017).